Interaction of water waves with an array of vertical cylinders using null-field integral equations

Jeng-Tzong Chen[1]

[1]Life-time Distinguished Professor, Department of Harbor and River Engineering,
National Taiwan Ocean University

Ying-Te Lee[2]

[2]Ph.D. Candidate, Department of Harbor and River Engineering,
National Taiwan Ocean University

Abstract

The scattering of water waves by an array of vertical circular cylinders is solved by using the null-field integral equations in conjunction with degenerate kernels and Fourier series to avoid calculating the Cauchy and Hadamard principal values. In the implementation, the null-field point can be exactly located on the real boundary owing to the introduction of degenerate kernels for fundamental solutions. An adaptive observer system of polar coordinate is considered to fully employ the property of degenerate kernels. For the hypersingular equation, vector decomposition for the radial and tangential gradients is carefully considered. This method can be seen as a semi-analytical approach since errors attribute from the truncation of Fourier series. Neither hypersingularity in the Burton and Miller approach nor the CHIEF concepts were required to deal with the problem of irregular frequencies. Four gains, well-posed model, singularity free, boundary-layer effect free and exponential convergence are achieved using the present approach. Numerical results are given for the forces and free-surface elevation around the circular boundaries. A general-purpose program for water wave impinging several circular cylinders with arbitrary number, radius, and position was developed. One example of water wave-structure interaction by an array of four bottom-mounted cylinders was demonstrated to see the validity of the present formulation and was compared with those of Linton and Evans, and Perrey-Debain *et al*.

Keywords: null-field integral equation, degenerate kernel, Fourier series, Helmholtz, radiation, scattering

1. Introduction

Over the past forty years, several numerical methods including finite difference, finite element and boundary element methods, were employed to solve a wide range of problems in ocean engineering. There is considerable interest for countries with long coasts, *e.g*., USA, Japan and Taiwan. It is well known that boundary integral equation methods have been used to solve radiation and scattering problems for many years. The importance of the integral equation in the solution, both theoretical and practical, for certain types of boundary value problems is universally recognized. One of the problems frequently addressed in BIEM/BEM is the problem of irregular frequencies in boundary integral formulations for exterior acoustics and water wave problems. These frequencies do not represent any kind of physical resonance but are due to the numerical method, which has non-unique solutions at characteristic frequencies associated with the eigenfrequency of the interior problem. Burton and

Miller approach [1] as well as CHIEF technique [2] have been employed to deal with these problems.

Regarding to the irregular frequency, a large amount of papers on acoustics have been published. For example, numerical examples for non-uniform radiation and scattering problems by using the dual BEM were provided and the irregular frequencies were easily found [3]. The non-uniqueness of radiation and scattering problems are numerically manifested in a rank deficiency of the influence coefficient matrix in BEM [1]. In order to obtain the unique solution, several integral equation formulations that provide additional constraints to the original system of equations have been proposed. Burton and Miller [1] proposed an integral equation that was valid for all wave numbers by forming a linear combination of the singular integral equation and its normal derivative. However, the calculation for the hypersingular integration is required. To avoid the computation of hypersingularity, an alternative method, Schenck [2] used the CHIEF method, which employs the boundary integral equations by

collocating the interior point as an auxiliary condition to make up deficient constraint condition. Many researchers [4-6] applied the CHIEF method to deal with the problem of fictitious frequencies. If the chosen point locates on the nodal line of the associated interior eigenproblem, then this method fails. To overcome this difficulty, Wu and Seybert [4, 5] employed a CHIEF-block method using the weighted residual formulation for acoustic problems. On the contrary, only a few papers on water wave can be found. For water wave problems, Ohmatsu [7] presented a combined integral equation method (CIEM), it was similar to the CHIEF-block method for acoustics proposed by Wu and Seybert. In the CIEM, two additional constraints for one interior point result in an overdetermined system to insure the removal of irregular frequencies. An enhanced CHIEF method was also proposed by Lee and Wu [6]. The main concern of the CHIEF method is how many numbers of interior points are selected and where the positions should be located. Recently, the appearance of irregular frequency in the method of fundamental solutions was theoretically proved and numerically implemented [8]. However, as far as the present authors are aware, only a few papers have been published to date reporting on the efficacy of these methods in radiation and scattering problems involving more than one vibrating body. For example, Dokumaci and Sarigül [9] discussed the fictitious frequency of radiation problem of two spheres. They used the surface Helmholtz integral equation (SHIE) and the CHIEF method to find the position of fictitious frequency. In our formulation, we are also concerned with the fictitious frequency especially for the multiple cylinders of scatters and radiators. We may wonder if there is one approach free of both Burton and Miller approach and CHIEF technique to deal with irregular frequencies.

For the problems with circular boundaries, the Fourier series expansion method is specially suitable to obtain the analytical solution. The interaction of water waves with arrays of vertical circular cylinders was studied using the dispersion relation by Linton and Evans [10]. If the depth dependence is removed, it also becomes two-dimensional Helmholtz problem in a similar way of acoustics. For membrane and plate problems, analytical treatments of integral equations for circular and annular domains were proposed in closed-form expressions for the integral in terms of Fourier coefficients by Kitahara [11]. Elsherbeni and Hamid [12] used the method of moments to solve the scattering problem by parallel conducting circular cylinders. They also divided the total scattered field into two components, namely a noninteraction term and a term due to all interactions between the cylinders. Chen *et al.* [3] employed the dual BEM to solve the exterior acoustic problems with circular boundary. Grote and Kirsch [13] utilized multiple Dirichlet to Neumann (DtN) method to solve multiple scattering problems of cylinders. DtN solution was obtained by combining contributions from multiple outgoing wave fields. Degenerate kernels were given in the book of Kress [14]. The mathematical proof of exponential convergence for Helmholtz problems using the Fourier expansion was derived in [15]. According to the literature review, it is observed that exact solutions for boundary value problems are only limited for simple cases, *e.g.* a cylinder radiator and scatter, half-plane with a semi-circular canyon, a hole under half-plane, two holes in an infinite plate. Therefore, proposing a systematic approach for solving BVP with circular boundaries of various numbers, positions and radii is our goal in this article.

Following the success of our experiences on Laplace and biharmonic problems, we extend the null-field boundary integral equation method (BIEM) to solve the scattering problems of water wave across an array of circular cylinders. To fully utilize the geometry of circular boundary, not only Fourier series for boundary densities as previously used by many researchers but also the degenerate kernel for fundamental solutions in the present formulation is incorporated into the null-field integral equation. All the improper boundary integrals are free of calculating the principal values (Cauchy and Hadamard) in place of series sum. In analytically integrating each circular boundary for the null-field equation, the adaptive observer system of polar coordinate is considered to fully employ the property of degenerate kernel. To avoid double integration in the Galerkin sense, point collocation approach is considered. Free of worrying how to choose the collocation points, uniform collocation along the circular boundary yields a well-posed matrix. For the hypersingular equation, vector decomposition for the radial and tangential gradients is carefully considered, especially for the eccentric case. Finally, problem of water wave-structure interaction by an array of four bottom-mounted cylinders was solved to

demonstrate the validity of the present method. The results are compared with those of the analytical solution derived by Linton and Evan [10], and numerical solution of plane wave BEM by Perrey-Debain *et al*. [16].

2. Problem statement and integral formulation

2.1 Problem statement

Based on the linear water wave theory, there exists a velocity potential $\Phi(x, y, z, t)$ where (x, y) in plane and z is the vertical direction. Now we assume N vertical cylinders mounted at $z = -h$ upward to the free surface as shown in Figure 1. The governing equation of the water
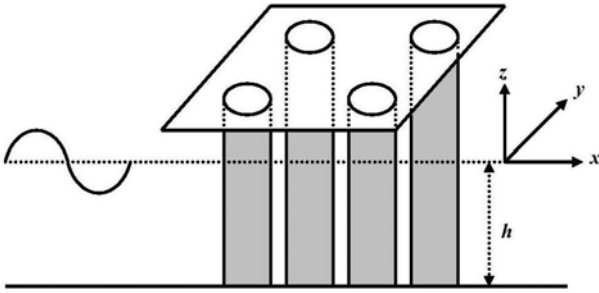

Figure 1 Problem statement of water waves with an array of vertical cylinders

wave problem is the Laplace equation

$$\nabla^2 \Phi(x, y, z; t) = 0, \quad (x, y, z) \in D . \tag{1}$$

Using the technique of separation variable for space and time, we have

$$\Phi(x, y, z, t) = \text{Re}\{\phi(x, y) f(z) e^{-i\omega t}\}, \tag{2}$$

where

$$f(z) = \frac{-igA}{\omega} \frac{\cosh k(z + h)}{\cosh kh}, \tag{3}$$

to satisfy boundary conditions of seabed and free-surface conditions as shown below:

$$-\frac{\partial \Phi}{\partial n} = 0, \quad z = -h(x, y), \tag{4}$$

$$-\Phi_z = H_t - \Phi_z H_x - \Phi_y H_y,$$
$$z = H(x, y, t). \tag{5}$$

Substituting Eq.(2) into Eq.(1), we have

$$(\nabla^2 + k^2)\phi(x, y) = 0, \quad (x, y) \in D , \tag{6}$$

where ∇^2, k and D are the Laplacian operator, the wave number, and the domain of interest, respectively. Rigid cylinders yield the Neumann boundary conditions as shown below:

$$\frac{\partial \phi(x, y)}{\partial n} = 0, \quad (x, y) \in B \tag{7}$$

The dispersion relation is shown below:

$$k \tanh kh = K \equiv \frac{\omega^2}{g}, \tag{8}$$

The free surface elevation is defined by

$$H(x, y, t) = \text{Re}\{\eta(x, y) e^{-i\omega t}\} \tag{9}$$

where

$$\eta(x, y) = A\phi(x, y) \tag{10}$$

in which A represents the amplitude of incident wave of angle β as shown below:

$$\phi_I(x, y) = e^{ik(x \cos \beta + y \sin \beta)} \equiv e^{ikr \cos(\theta - \beta)} . \tag{11}$$

The dynamic pressure can be obtained by

$$p = -\rho \frac{\partial \Phi}{\partial t}$$
$$= \rho gA \frac{\cosh k(z + h)}{\cosh kh} \phi(x, y) e^{-iwt} . \tag{12}$$

The two components of the first-order force X^j on the jth cylinder is given by integrating the pressure over the circular boundary as shown below:

$$X^j = -\frac{\rho gAa_j}{k} \tanh kh \int_0^{2\pi} \phi(x, y) \begin{Bmatrix} \cos \theta_j \\ \sin \theta_j \end{Bmatrix} d\theta_j, \tag{13}$$

where a_j denotes the radius of the jth cylinder.

2.2 Dual boundary integral formulation

Based on the dual boundary integral formulation of the domain point [17], we have

$$2\pi u(\mathbf{x}) = \int_B T^I(\mathbf{s}, \mathbf{x}) u(\mathbf{s}) dB(\mathbf{s})$$
$$- \int_B U^I(\mathbf{s}, \mathbf{x}) t(\mathbf{s}) dB(\mathbf{s}), \quad \mathbf{x} \in D \cup B, \tag{14}$$

$$2\pi t(\mathbf{x}) = \int_B M^I(\mathbf{s}, \mathbf{x}) u(\mathbf{s}) dB(\mathbf{s})$$
$$- \int_B L^I(\mathbf{s}, \mathbf{x}) t(\mathbf{s}) dB(\mathbf{s}), \quad \mathbf{x} \in D \cup B, \tag{15}$$

where $\mathbf{s}$ and $\mathbf{x}$ are the source and field points, respectively, B is the boundary. Equations (14) and (15) are quite different from the conventional formulation since they are valid not only for the point in the domain D but also for the boundary points if the kernels are properly expressed as the interior (superscript *I*) degenerate kernels. The set of $\mathbf{x}$ in Eqs.(14) and (15) is closed since $x \in D \cup B$. The flux $t(\mathbf{s})$ is the directional derivative of $u(\mathbf{s})$ along the outer normal direction at $\mathbf{s}$. For the interior point, $t(\mathbf{x})$ is artificially defined. For example, $t(\mathbf{x}) = \partial u(\mathbf{x})/\partial x_1$, if $\mathbf{n} = (1,0)$ and $t(\mathbf{x}) = \partial u(\mathbf{x})/\partial x_2$, if $\mathbf{n} = (0,1)$ where (x_1, x_2) is the coordinate of the field point $\mathbf{x}$. The $U(\mathbf{s},\mathbf{x})$, $T(\mathbf{s},\mathbf{x})$, $L(\mathbf{s},\mathbf{x})$ and $M(\mathbf{s},\mathbf{x})$ represent the four kernel functions [3]

$$U(\mathbf{s}, \mathbf{x}) = \frac{-i\pi H_0^{(1)}(kr)}{2}, \qquad (16)$$

$$T(\mathbf{s}, \mathbf{x}) = \frac{\partial U(\mathbf{s}, \mathbf{x})}{\partial \mathbf{n}_s}, \qquad (17)$$

$$L(\mathbf{s}, \mathbf{x}) = \frac{\partial U(\mathbf{s}, \mathbf{x})}{\partial \mathbf{n}_x}, \qquad (18)$$

$$M(\mathbf{s}, \mathbf{x}) = \frac{\partial U(\mathbf{s}, \mathbf{x})}{\partial \mathbf{n}_s \partial \mathbf{n}_x}, \qquad (19)$$

where $H_n^{(1)}(kr) = J_n(kr) + iY_n(kr)$ is the n-th order Hankel function of the first kind, J_n is the Bessel function, Y_n is the modified Bessel function, $r = |\mathbf{x} - \mathbf{s}|$, $y_i = s_i - x_i$, $i^2 = -1$, n_i and $\bar{n}_i$ are the i-th components of the outer normal vectors at $\mathbf{s}$ and $\mathbf{x}$, respectively. Equations (14) and (15) are referred to singular and hypersingular boundary integral equations (BIEs), respectively.

2.3 Null-field integral formulation in conjunction with the degenerate kernel and Fourier series

By collocating $\mathbf{x}$ outside the domain ($\mathbf{x} \in D^c$, complementary domain), we obtain the null-field integral equations as shown below [18]:

$$0 = \int_B T^E(\mathbf{s}, \mathbf{x})u(\mathbf{s})dB(\mathbf{s})$$
$$-\int_B U^E(\mathbf{s}, \mathbf{x})t(\mathbf{s})dB(\mathbf{s}), \quad \mathbf{x} \in D^c \cup B, \qquad (20)$$

$$0 = \int_B M^E(\mathbf{s}, \mathbf{x})u(\mathbf{s})dB(\mathbf{s})$$
$$-\int_B L^E(\mathbf{s}, \mathbf{x})t(\mathbf{s})dB(\mathbf{s}), \quad \mathbf{x} \in D^c \cup B, \qquad (21)$$

where the collocation point $\mathbf{x}$ can locate on the outside of the domain as well as B if kernels are substituted into proper exterior (superscript, E) degenerate kernels. Since degenerate kernels can describe the fundamental solutions in two regions (interior and exterior domains), the BIE for the domain point of Eqs.(14) and (15) and null-field BIE of Eqs.(20) and (21) can include the boundary point. In real implementation, the null-field point can be pushed on the real boundary since we introduce the expression of degenerate kernel for fundamental solutions. By using the polar coordinate, we can express $\mathbf{x} = (\rho, \phi)$ and $\mathbf{s} = (R, \theta)$. The four kernels U, T, L and M can be expressed in terms of degenerate kernels as shown below [3]:

$$U(\mathbf{s}, \mathbf{x}) = \begin{cases} U^I(\mathbf{s}, \mathbf{x}) = \dfrac{-\pi i}{2} \displaystyle\sum_{m=0}^{\infty} \varepsilon_m J_m(k\rho)H_m^{(1)}(kR)\cos(m(\theta - \phi)), & R \geq \rho, \\[2mm] U^E(\mathbf{s}, \mathbf{x}) = \dfrac{-\pi i}{2} \displaystyle\sum_{m=0}^{\infty} \varepsilon_m H_m^{(1)}(k\rho)J_m(kR)\cos(m(\theta - \phi)), & R < \rho, \end{cases} \qquad (22)$$

$$T(\mathbf{s}, \mathbf{x}) = \begin{cases} T^I(\mathbf{s}, \mathbf{x}) = \dfrac{-\pi ki}{2} \displaystyle\sum_{m=0}^{\infty} \varepsilon_m J_m(k\rho)H_m'^{(1)}(kR)\cos(m(\theta - \phi)), & R > \rho, \\[2mm] T^E(\mathbf{s}, \mathbf{x}) = \dfrac{-\pi ki}{2} \displaystyle\sum_{m=0}^{\infty} \varepsilon_m H_m^{(1)}(k\rho)J_m'(kR)\cos(m(\theta - \phi)), & R < \rho, \end{cases} \qquad (23)$$

$$L(\mathbf{s}, \mathbf{x}) = \begin{cases} L^I(\mathbf{s}, \mathbf{x}) = \dfrac{-\pi ki}{2} \displaystyle\sum_{m=0}^{\infty} \varepsilon_m J_m'(k\rho)H_m^{(1)}(kR)\cos(m(\theta - \phi)), & R > \rho, \\[2mm] L^E(\mathbf{s}, \mathbf{x}) = \dfrac{-\pi ki}{2} \displaystyle\sum_{m=0}^{\infty} \varepsilon_m H_m'^{(1)}(k\rho)J_m(kR)\cos(m(\theta - \phi)), & R < \rho, \end{cases} \qquad (24)$$

$$M(\mathbf{s}, \mathbf{x}) = \begin{cases} M^I(\mathbf{s}, \mathbf{x}) = \dfrac{-\pi k^2 i}{2} \displaystyle\sum_{m=0}^{\infty} \varepsilon_m J_m'(k\rho)H_m'^{(1)}(kR)\cos(m(\theta - \phi)), & R \geq \rho, \\[2mm] M^E(\mathbf{s}, \mathbf{x}) = \dfrac{-\pi k^2 i}{2} \displaystyle\sum_{m=0}^{\infty} \varepsilon_m H_m'^{(1)}(k\rho)J_m'(kR)\cos(m(\theta - \phi)), & R < \rho. \end{cases} \qquad (25)$$

where ε_m is the Neumann factor

$$\varepsilon_m = \begin{cases} 1, & m = 0, \\ 2, & m = 1, 2, \Lambda, \infty. \end{cases} \quad (26)$$

Mathematically speaking, the expressions of fundamental solutions in Eqs.(22)-(26) are termed degenerate kernels (or separable kernels) which can expand to sums of products of function of the field point **x** alone by functions of the source point **s** alone. If the finite sum of series is considered, the kernel is finite rank. As we shall see in the later sections, the theory of boundary integral equations with degenerate kernel is nothing more than the linear algebra. Since the potentials resulted from $T(\mathbf{s},\mathbf{x})$ and $L(\mathbf{s},\mathbf{x})$ are discontinuous across the boundary, the potentials of $T(\mathbf{s},\mathbf{x})$ and $L(\mathbf{s},\mathbf{x})$ for $R \to \rho^+$ and $R \to \rho^-$ are different. This is the reason why $R = \rho$ is not included in the expression for the degenerate kernels of $T(\mathbf{s},\mathbf{x})$ and $L(\mathbf{s},\mathbf{x})$. The degenerate kernels simply serve as the means to evaluate regular integrals analytically and take the limits analytically. The reason is that Eqs.(14) and (20) yield the same algebraic equation when the limit is taken from the inside or from the outside of the region. Both limits represent the same algebraic equation that is an approximate counterpart of the boundary integral equation, that for the case of a smooth boundary has in the left-hand side term $\pi u(\mathbf{x})$ or $\pi t(\mathbf{x})$ rather than $2\pi u(\mathbf{x})$ or $2\pi t(\mathbf{x})$ for the domain point or 0 for the point outside the domain. Besides, the limiting case to the boundary is also addressed. The continuous and jump behavior across the boundary is well captured by the Wronskian property of Bessel function J_m and Y_m bases

$$W(J_m(kR), Y_m(kR))$$
$$= Y'_m(kR)J_m(kR) - Y_m(kR)J'_m(kR) = \frac{2}{\pi k R} \quad (27)$$

as shown below

$$\int_0^{2\pi} \left(T^I(\mathbf{s},\mathbf{x}) - T^E(\mathbf{s},\mathbf{x}) \right) \cos(m\theta) R d\theta$$
$$= 2\pi \cos(m\phi), \quad \mathbf{x} \in B, \quad (28)$$

$$\int_0^{2\pi} \left(T^I(\mathbf{s},\mathbf{x}) - T^E(\mathbf{s},\mathbf{x}) \right) \sin(m\theta) R d\theta$$
$$= 2\pi \sin(m\phi), \quad \mathbf{x} \in B. \quad (29)$$

where T^I and T^E are the interior and exterior expressions for the T kernel in the degenerate form. After employing Eqs.(28) and (29), Eq.(14) and Eq.(20) yield the same linear algebraic equation

when **x** is exactly pushed on the boundary from the domain or the complementing domain. A proof for the Laplace case can be found [18].

In order to fully utilize the geometry of circular boundary, the potential $u(\mathbf{s})$ and its normal flux $t(\mathbf{s})$ can be approximated by employing the Fourier series. Therefore, we obtain

$$u(\mathbf{s}) = a_0 + \sum_{n=1}^{\infty} (a_n \cos n\theta + b_n \sin n\theta) \quad (30)$$

$$t(\mathbf{s}) = p_0 + \sum_{n=1}^{\infty} (p_n \cos n\theta + q_n \sin n\theta) \quad (31)$$

where a_0, a_n, b_n, p_0, p_n and q_n are the Fourier coefficients and θ is the polar angle which is equally discretized. Equations (20) and (21) can be easily calculated by employing the orthogonal property of Fourier series. In the real computation, only the finite P terms are used in the summation of Eqs.(30) and (31).

2.4 Adaptive observer system

Since the boundary integral equations are frame indifferent, *i.e.* rule of objectivity is obeyed. Adaptive observer system is chosen to fully employ the property of degenerate kernels. Figure 2 shows the boundary integration for the circular boundaries. It is worthy noted that the origin of the observer system can be adaptively located on the center of the corresponding circle under integration to fully utilize the geometry of circular boundary. The dummy variable in the integration on the circular boundary is just the angle (θ) instead of the radial coordinate (R). By using the adaptive system, all
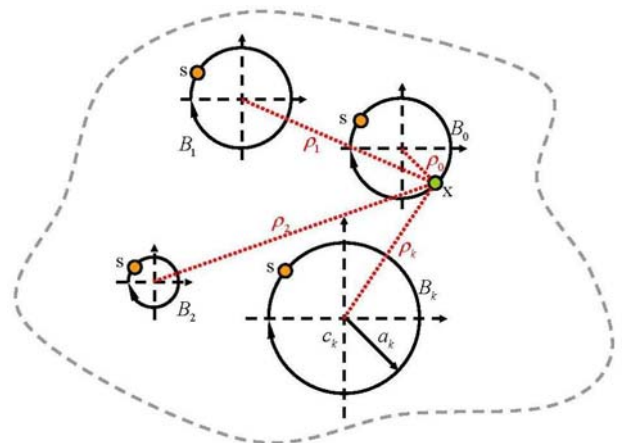

Figure 2 The adaptive observer system

the boundary integrals can be determined analytically free of principal value.

2.5 Vector decomposition technique for the potential gradient in the hypersingular formulation

Since hypersingular equation plays an important role for dealing with fictitious frequencies, potential gradient of the field quantity is required to calculate. For the eccentric case, the field point and source point may not locate on the circular boundaries with the same center except the two points on the same circular boundary or on the annular cases. Special treatment for the normal derivative should be taken care. As shown in Figure 3 where the origins of observer system are different,
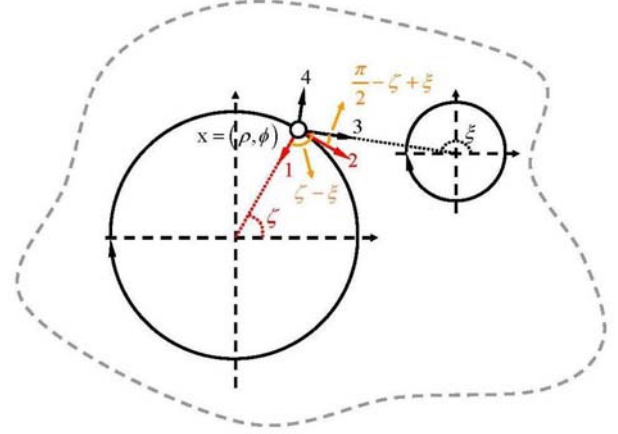
Figure 3 Vector decomposition technique for the potential gradient in the hypersingular equation

the true normal direction $\hat{e}_1$ with respect to the collocation point $\mathbf{x}$ on the B_j boundary should be superimposed by using the radial direction $\hat{e}_3$ and angular direction $\hat{e}_4$. We call this treatment "vector decomposition technique". According to the concept, Eqs.(24) and (25) can be modified as

$$
L(\mathbf{s},\mathbf{x}) =
\begin{cases}
L^I(\mathbf{s},\mathbf{x}) = \dfrac{-\pi k i}{2}\sum_{m=0}^{\infty}\varepsilon_m J'_m(k\rho)H_m^{(1)}(kR)\cos(m(\theta-\phi))\cos(\zeta-\xi) \\
\qquad -\dfrac{\pi m i}{2\rho}\sum_{m=0}^{\infty}\varepsilon_m J_m(k\rho)H_m^{(1)}(kR)\sin(m(\theta-\phi))\sin(\zeta-\xi), \quad R>\rho, \\
L^E(\mathbf{s},\mathbf{x}) = \dfrac{-\pi k i}{2}\sum_{m=0}^{\infty}\varepsilon_m H'^{(1)}_m(k\rho)J_m(kR)\cos(m(\theta-\phi))\cos(\zeta-\xi) \\
\qquad -\dfrac{\pi m i}{2\rho}\sum_{m=0}^{\infty}\varepsilon_m H_m^{(1)}(k\rho)J_m(kR)\sin(m(\theta-\phi))\sin(\zeta-\xi), \quad R<\rho,
\end{cases}
\tag{32}
$$

$$
M(\mathbf{s},\mathbf{x}) =
\begin{cases}
M^I(\mathbf{s},\mathbf{x}) = \dfrac{-\pi k^2 i}{2}\sum_{m=0}^{\infty}\varepsilon_m J'_m(k\rho)H'^{(1)}_m(kR)\cos(m(\theta-\phi))\cos(\zeta-\xi) \\
\qquad -\dfrac{\pi m k i}{2\rho}\sum_{m=0}^{\infty}\varepsilon_m J_m(k\rho)H'^{(1)}_m(kR)\sin(m(\theta-\phi))\sin(\zeta-\xi), \quad R\geq\rho, \\
M^E(\mathbf{s},\mathbf{x}) = \dfrac{-\pi k^2 i}{2}\sum_{m=0}^{\infty}\varepsilon_m H'^{(1)}_m(k\rho)J'_m(kR)\cos(m(\theta-\phi))\cos(\zeta-\xi) \\
\qquad -\dfrac{\pi m k i}{2\rho}\sum_{m=0}^{\infty}\varepsilon_m H_m^{(1)}(k\rho)J'_m(kR)\sin(m(\theta-\phi))\sin(\zeta-\xi), \quad R<\rho,
\end{cases}
\tag{33}
$$

2.6 Linear Algebraic Equation

In order to calculate the $2P+1$ unknown Fourier coefficients, $2P+1$ boundary points on each circular boundary are needed to be collocated. By collocating the null-field point exactly on the *kth* circular boundary for Eqs.(20) and (21) as shown in Figure 2, we have

$$
0 = \sum_{j=1}^{N}\int_{B_j} T^E(\mathbf{s},\mathbf{x}_k)u(\mathbf{s})dB(\mathbf{s})
$$
$$
-\sum_{j=1}^{N}\int_{B_j} U^E(\mathbf{s},\mathbf{x}_k)t(\mathbf{s})dB(\mathbf{s}), \quad \mathbf{x}_k\in D^c\cup B,
\tag{34}
$$

$$
0 = \int_B M^E(\mathbf{s},\mathbf{x}_k)u(\mathbf{s})dB(\mathbf{s})
$$
$$
-\int_B L^E(\mathbf{s},\mathbf{x}_k)t(\mathbf{s})dB(\mathbf{s}), \quad \mathbf{x}_k\in D^c\cup B,
\tag{35}
$$

where N is the number of circles. It is noted

that the path is anticlockwise for the outer circle. Otherwise, it is clockwise. For the B_j integral of the circular boundary, the kernels of $U(\mathbf{s},\mathbf{x})$, $T(\mathbf{s},\mathbf{x})$, $L(\mathbf{s},\mathbf{x})$ and $M(\mathbf{s},\mathbf{x})$ are respectively expressed in terms of degenerate kernels of Eqs. (22), (23), (32) and (33) with respect to the observer origin at the center of B_j. The boundary densities of $u(\mathbf{s})$ and $t(\mathbf{s})$ are substituted by using the Fourier series of Eqs. (30) and (31), respectively. In the B_j integration, we set the origin of the observer system to collocate at the center c_j of B_j to fully utilize the degenerate kernel and Fourier series. By locating the null-field point on the real boundary B_k from outside of the domain D^E in numerical implementation, a linear algebraic system is obtained

$$[\mathbf{U}]\{\mathbf{t}\} = [\mathbf{T}]\{\mathbf{u}\}, \tag{36}$$

$$[\mathbf{L}]\{\mathbf{t}\} = [\mathbf{M}]\{\mathbf{u}\}, \tag{37}$$

where $[\mathbf{U}]$, $[\mathbf{T}]$, $[\mathbf{L}]$ and $[\mathbf{M}]$ are the influence matrices with a dimension of $N \times (2P+1)$ by $N \times (2P+1)$, and $\{\mathbf{t}\}$ and $\{\mathbf{u}\}$ denote the vectors for $t(\mathbf{s})$ and $u(\mathbf{s})$ of the Fourier coefficients with a dimension of $N \times (2P+1)$ by 1, in which, $[\mathbf{U}]$, $[\mathbf{T}]$, $[\mathbf{L}]$, $[\mathbf{M}]$, $\{\mathbf{u}\}$ and $\{\mathbf{t}\}$ can be defined as follows:

$$[\mathbf{U}] = [\mathbf{U}_{\alpha\beta}] = \begin{bmatrix} \mathbf{U}_{11} & \mathbf{U}_{12} & \Lambda & \mathbf{U}_{1N} \\ \mathbf{U}_{21} & \mathbf{U}_{22} & \Lambda & \mathbf{U}_{2N} \\ M & M & O & M \\ \mathbf{U}_{N1} & \mathbf{U}_{N2} & \Lambda & \mathbf{U}_{NN} \end{bmatrix}, \tag{38}$$

$$[\mathbf{T}] = [\mathbf{T}_{\alpha\beta}] = \begin{bmatrix} \mathbf{T}_{11} & \mathbf{T}_{12} & \Lambda & \mathbf{T}_{1N} \\ \mathbf{T}_{21} & \mathbf{T}_{22} & \Lambda & \mathbf{T}_{2N} \\ M & M & O & M \\ \mathbf{T}_{N1} & \mathbf{T}_{N2} & \Lambda & \mathbf{T}_{NN} \end{bmatrix}, \tag{39}$$

$$[\mathbf{L}] = [\mathbf{L}_{\alpha\beta}] = \begin{bmatrix} \mathbf{L}_{11} & \mathbf{L}_{12} & \Lambda & \mathbf{L}_{1N} \\ \mathbf{L}_{21} & \mathbf{L}_{22} & \Lambda & \mathbf{L}_{2N} \\ M & M & O & M \\ \mathbf{L}_{N1} & \mathbf{L}_{N2} & \Lambda & \mathbf{L}_{NN} \end{bmatrix} \tag{40}$$

$$[\mathbf{M}] = [\mathbf{M}_{\alpha\beta}] = \begin{bmatrix} \mathbf{M}_{11} & \mathbf{M}_{12} & \Lambda & \mathbf{M}_{1N} \\ \mathbf{M}_{21} & \mathbf{M}_{22} & \Lambda & \mathbf{M}_{2N} \\ M & M & O & M \\ \mathbf{M}_{N1} & \mathbf{M}_{N2} & \Lambda & \mathbf{M}_{NN} \end{bmatrix} \tag{41}$$

$$\{\mathbf{u}\} = \begin{Bmatrix} \mathbf{u}_1 \\ \mathbf{u}_2 \\ M \\ \mathbf{u}_N \end{Bmatrix}, \quad \{\mathbf{t}\} = \begin{Bmatrix} \mathbf{t}_1 \\ \mathbf{t}_2 \\ M \\ \mathbf{t}_N \end{Bmatrix} \tag{42}$$

where the vectors $\{\mathbf{u}_k\}$ and $\{\mathbf{t}_k\}$ are in the form of $\{a_0^k \ a_1^k \ b_1^k \Lambda \ a_p^k \ b_p^k\}^T$ and $\{p_0^k \ p_1^k \ q_1^k \Lambda \ p_p^k \ q_p^k\}^T$; the first subscript "$\alpha$" ($\alpha$ =1, 2, …, N) in the $[\mathbf{U}_{\alpha\beta}]$ denotes the index of the αth circle where the collocation point is located and the second subscript "β" (β =1, 2, …, N) denotes the index of the βth circle where the boundary data $\{\mathbf{u}_k\}$ or $\{\mathbf{t}_k\}$ are specified. The number of circular holes is N and the highest harmonic of truncated terms is P. The coefficient matrix of the linear algebraic system is partitioned into blocks, and each diagonal block ($\mathbf{U}_{pp}$) corresponds to the influence matrices due to the same circle of collocation and Fourier expansion. After uniformly collocating the point along the αth circular boundary, the sub-matrix can be written as

$$[\mathbf{U}_{\alpha\beta}] = \begin{bmatrix} U_{\alpha\beta}^{0c}(\phi_1) & U_{\alpha\beta}^{1c}(\phi_1) & U_{\alpha\beta}^{1s}(\phi_1) & \Lambda & U_{\alpha\beta}^{Pc}(\phi_1) & U_{\alpha\beta}^{Ps}(\phi_1) \\ U_{\alpha\beta}^{0c}(\phi_2) & U_{\alpha\beta}^{1c}(\phi_2) & U_{\alpha\beta}^{1s}(\phi_2) & \Lambda & U_{\alpha\beta}^{Pc}(\phi_2) & U_{\alpha\beta}^{Ps}(\phi_2) \\ U_{\alpha\beta}^{0c}(\phi_3) & U_{\alpha\beta}^{1c}(\phi_3) & U_{\alpha\beta}^{1s}(\phi_3) & \Lambda & U_{\alpha\beta}^{Pc}(\phi_3) & U_{\alpha\beta}^{Ps}(\phi_3) \\ M & M & M & O & M & M \\ U_{\alpha\beta}^{0c}(\phi_{2P}) & U_{\alpha\beta}^{1c}(\phi_{2P}) & U_{\alpha\beta}^{1s}(\phi_{2P}) & \Lambda & U_{\alpha\beta}^{Pc}(\phi_{2P}) & U_{\alpha\beta}^{Ps}(\phi_{2P}) \\ U_{\alpha\beta}^{0c}(\phi_{2P+1}) & U_{\alpha\beta}^{1c}(\phi_{2P+1}) & U_{\alpha\beta}^{1s}(\phi_{2P+1}) & \Lambda & U_{\alpha\beta}^{Pc}(\phi_{2P+1}) & U_{\alpha\beta}^{Ps}(\phi_{2P+1}) \end{bmatrix} \tag{43}$$

$$[\mathbf{T}_{\alpha\beta}] = \begin{bmatrix} T_{\alpha\beta}^{0c}(\phi_1) & T_{\alpha\beta}^{1c}(\phi_1) & T_{\alpha\beta}^{1s}(\phi_1) & \Lambda & T_{\alpha\beta}^{Pc}(\phi_1) & T_{\alpha\beta}^{Ps}(\phi_1) \\ T_{\alpha\beta}^{0c}(\phi_2) & T_{\alpha\beta}^{1c}(\phi_2) & T_{\alpha\beta}^{1s}(\phi_2) & \Lambda & T_{\alpha\beta}^{Pc}(\phi_2) & T_{\alpha\beta}^{Ps}(\phi_2) \\ T_{\alpha\beta}^{0c}(\phi_3) & T_{\alpha\beta}^{1c}(\phi_3) & T_{\alpha\beta}^{1s}(\phi_3) & \Lambda & T_{\alpha\beta}^{Pc}(\phi_3) & T_{\alpha\beta}^{Ps}(\phi_3) \\ M & M & M & O & M & M \\ T_{\alpha\beta}^{0c}(\phi_{2P}) & T_{\alpha\beta}^{1c}(\phi_{2P}) & T_{\alpha\beta}^{1s}(\phi_{2P}) & \Lambda & T_{\alpha\beta}^{Pc}(\phi_{2P}) & T_{\alpha\beta}^{Ps}(\phi_{2P}) \\ T_{\alpha\beta}^{0c}(\phi_{2P+1}) & T_{\alpha\beta}^{1c}(\phi_{2P+1}) & T_{\alpha\beta}^{1s}(\phi_{2P+1}) & \Lambda & T_{\alpha\beta}^{Pc}(\phi_{2P+1}) & T_{\alpha\beta}^{Ps}(\phi_{2P+1}) \end{bmatrix} \tag{44}$$

$$[\mathbf{L}_{\alpha\beta}] = \begin{bmatrix} L_{\alpha\beta}^{0c}(\phi_1) & L_{\alpha\beta}^{1c}(\phi_1) & L_{\alpha\beta}^{1s}(\phi_1) & \Lambda & L_{\alpha\beta}^{Pc}(\phi_1) & L_{\alpha\beta}^{Ps}(\phi_1) \\ L_{\alpha\beta}^{0c}(\phi_2) & L_{\alpha\beta}^{1c}(\phi_2) & L_{\alpha\beta}^{1s}(\phi_2) & \Lambda & L_{\alpha\beta}^{Pc}(\phi_2) & L_{\alpha\beta}^{Ps}(\phi_2) \\ L_{\alpha\beta}^{0c}(\phi_3) & L_{\alpha\beta}^{1c}(\phi_3) & L_{\alpha\beta}^{1s}(\phi_3) & \Lambda & L_{\alpha\beta}^{Pc}(\phi_3) & L_{\alpha\beta}^{Ps}(\phi_3) \\ M & M & M & O & M & M \\ L_{\alpha\beta}^{0c}(\phi_{2P}) & L_{\alpha\beta}^{1c}(\phi_{2P}) & L_{\alpha\beta}^{1s}(\phi_{2P}) & \Lambda & L_{\alpha\beta}^{Pc}(\phi_{2P}) & L_{\alpha\beta}^{Ps}(\phi_{2P}) \\ L_{\alpha\beta}^{0c}(\phi_{2P+1}) & L_{\alpha\beta}^{1c}(\phi_{2P+1}) & L_{\alpha\beta}^{1s}(\phi_{2P+1}) & \Lambda & L_{\alpha\beta}^{Pc}(\phi_{2P+1}) & L_{\alpha\beta}^{Ps}(\phi_{2P+1}) \end{bmatrix} \tag{45}$$

$$[\mathbf{M}_{\alpha\beta}] = \begin{bmatrix} M_{\alpha\beta}^{0c}(\phi_1) & M_{\alpha\beta}^{1c}(\phi_1) & M_{\alpha\beta}^{1s}(\phi_1) & \Lambda & M_{\alpha\beta}^{Pc}(\phi_1) & M_{\alpha\beta}^{Ps}(\phi_1) \\ M_{\alpha\beta}^{0c}(\phi_2) & M_{\alpha\beta}^{1c}(\phi_2) & M_{\alpha\beta}^{1s}(\phi_2) & \Lambda & M_{\alpha\beta}^{Pc}(\phi_2) & M_{\alpha\beta}^{Ps}(\phi_2) \\ M_{\alpha\beta}^{0c}(\phi_3) & M_{\alpha\beta}^{1c}(\phi_3) & M_{\alpha\beta}^{1s}(\phi_3) & \Lambda & M_{\alpha\beta}^{Pc}(\phi_3) & M_{\alpha\beta}^{Ps}(\phi_3) \\ M & M & M & O & M & M \\ M_{\alpha\beta}^{0c}(\phi_{2P}) & M_{\alpha\beta}^{1c}(\phi_{2P}) & M_{\alpha\beta}^{1s}(\phi_{2P}) & \Lambda & M_{\alpha\beta}^{Pc}(\phi_{2P}) & M_{\alpha\beta}^{Ps}(\phi_{2P}) \\ M_{\alpha\beta}^{0c}(\phi_{2P+1}) & M_{\alpha\beta}^{1c}(\phi_{2P+1}) & M_{\alpha\beta}^{1s}(\phi_{2P+1}) & \Lambda & M_{\alpha\beta}^{Pc}(\phi_{2P+1}) & M_{\alpha\beta}^{Ps}(\phi_{2P+1}) \end{bmatrix} \tag{46}$$

It is noted that the superscript "0s" in Eq.(29) disappears since $\sin(0\theta) = 0$, and the element of $[\mathbf{U}_{\alpha\beta}]$, $[\mathbf{T}_{\alpha\beta}]$, $[\mathbf{L}_{\alpha\beta}]$ and $[\mathbf{M}_{\alpha\beta}]$ are defined as

$$U_{\alpha\beta}^{nc} = \int_{B_k} U(s_k, x_m)\cos(n\theta_k)R_k d\theta_k , \tag{47}$$

$$U_{\alpha\beta}^{ns} = \int_{B_k} U(s_k, x_m)\sin(n\theta_k)R_k d\theta_k , \tag{48}$$

$$T_{\alpha\beta}^{nc} = \int_{B_k} T(s_k, x_m)\cos(n\theta_k)R_k d\theta_k , \tag{49}$$

$$T_{\alpha\beta}^{ns} = \int_{B_k} T(s_k, x_m)\sin(n\theta_k)R_k d\theta_k , \tag{50}$$

$$L_{\alpha\beta}^{nc} = \int_{B_k} L(s_k, x_m)\cos(n\theta_k)R_k d\theta_k , \tag{51}$$

$$L_{\alpha\beta}^{ns} = \int_{B_k} L(s_k, x_m)\sin(n\theta_k)R_k d\theta_k , \tag{52}$$

$$M_{\alpha\beta}^{nc} = \int_{B_k} M(s_k, x_m)\cos(n\theta_k)R_k d\theta_k , \tag{53}$$

$$M_{\alpha\beta}^{ns} = \int_{B_k} M(s_k, x_m)\sin(n\theta_k)R_k d\theta_k , \tag{54}$$

where $n = 1, 2, \Lambda, P$, ϕ_m ($n = 1, 2, \Lambda, 2P+1$) is the polar angle of the collocating points $\mathbf{x}_m$ along the boundary. After obtaining the unknown Fourier coefficients, the origin of observer system is set to c_j in the B_j integration as shown in Figure 4 to obtain the interior potential by employing Eq.(14).

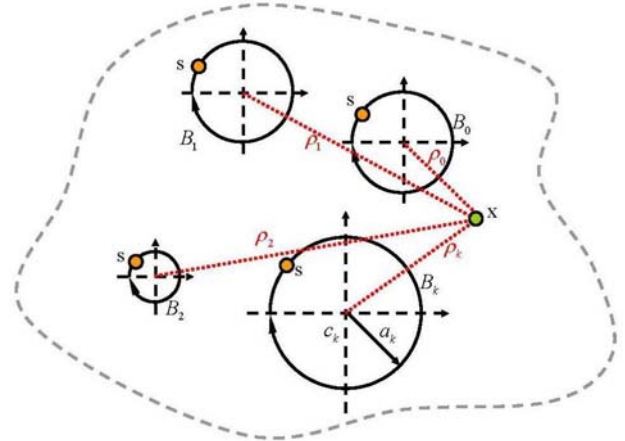The flowchart of the present method is shown in Figure 5.

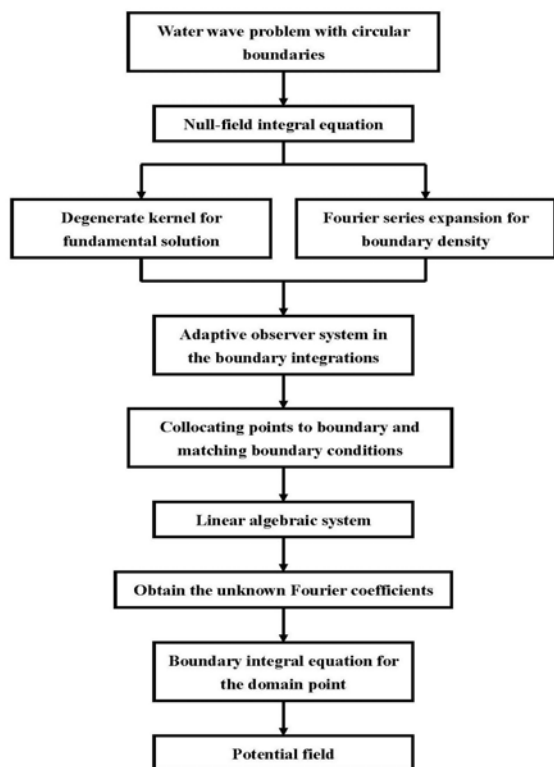**Figure 4 Sketch of the boundary integral equation for the domain point**

Figure 5 Flowchart of the present method

3. *An example: water wave impinging four cylinders*

In this example, we consider water wave structure problem by an array of four bottom-mounted vertical rigid circular cylinders with the same radius *a* located at the vertices of a square (-*b*,-*b*), (-*b*,*b*), (*b*,-*b*), (*b*,*b*), respectively, as shown in Figure 6. Consider the incident wave in the direction of 45 degrees. The first-order force for four cylinders in the direction of the incident wave
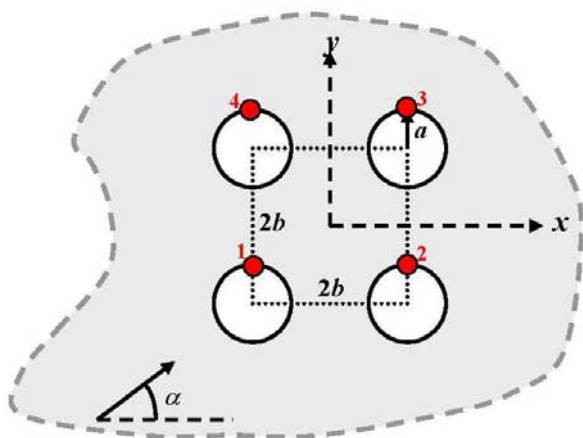

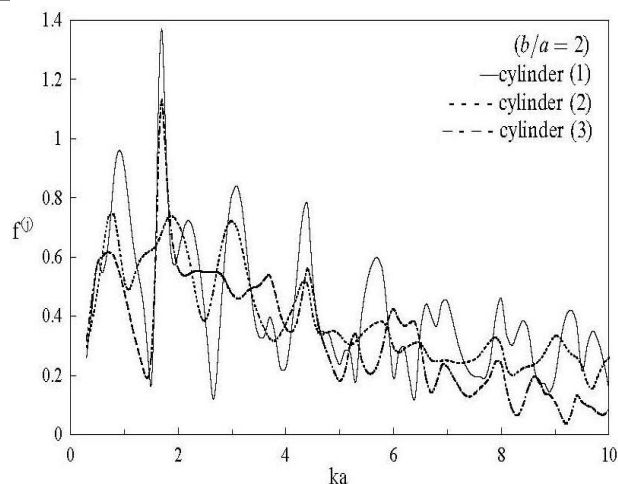Figure 6 Interaction of an incident water wave with four cylinders

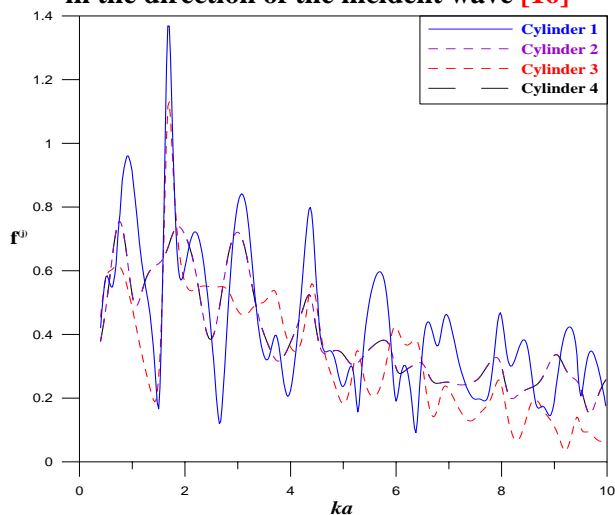Figure 7 The first-order force for four cylinders in the direction of the incident wave [16]

Figure 8 The first-order force for four cylinders using the proposed method

determined by Perrey-Debain *et al*. is shown in Figure 7 and the result of the present method is shown in Figure 8. It is found that the force effect on cylinder 2 and cylinder 4 is identical as expected due to symmetry. After comparing with the result of Perrey-Debain *et al*., good agreement is made. The maximum free-surface elevation amplitude is plotted in Figure 9. It agrees well with that of the plane wave BEM by Perrey-Debain *et al.* [16].

Table 1 Potential (ϕ) at the north pole of each cylinder ($ka = 1.7$)

|	**Present method**	**Perrey-Debain et al. [16]**	**Linton and Evan [10]**
Cylinder 1	-2.418395851 + i 0.753719467	-2.418395682 + i 0.753719398	-2.418395683 + i 0.753719398
Cylinder 2	2.328927362 – i 0.310367580	2.328927403 – i 0.310367705	2.328927400 – i 0.310367707
Cylinder 3	0.350612027 – i 0.198852116i	0.350611956 – i 0.198852086	0.350611956 – i 0.198852086
Cylinder 4	-0.383803194 + i 1.292792513i	-0.383803273 + i 1.292792457	-0.383803272 + i 1.292792455
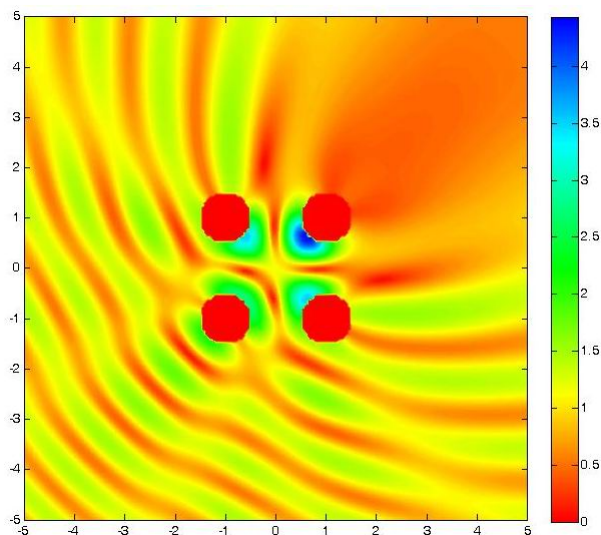
Figure 9 Contour of the maximum free-surface elevation amplitude

Figure 10 Absolute value of potential at the north pole versus the parameter ka

Also, the results of potentials at the north pole of each cylinder are also compared well with the approximate series given by Linton and Evans [10] and the BEM data by Perrey-Debain et al. [16] as shown in Table 1. The existence of the irregular frequencies is also examined. Figure 10 is shown the absolute value of the potential at the north pole on the Cylinder 4 versus the parameter ka. It is found that the irregular frequency does not occur. In the present approach, neither the Burton and Miller approach nor the CHIEF concepts were required to deal with the problem of irregular frequencies.
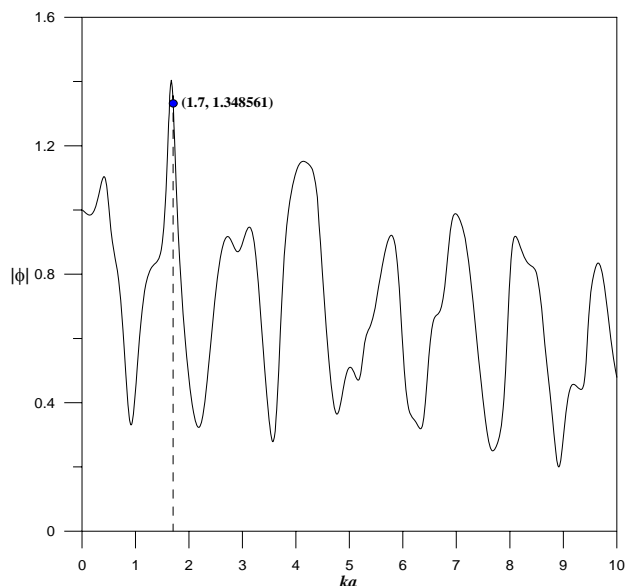
4. Conclusions

For the water wave scattering problems with circular cylinders, we have proposed a BIEM formulation by using degenerate kernels, null-field integral equation and Fourier series in companion with adaptive observer systems and vector decomposition. This method is a semi-analytical approach for Helmholtz problems with circular boundaries since only truncation error in the Fourier series is involved. The method shows great generality and versatility for the problems with multiple cylinders of arbitrary radii and positions. Fictitious frequencies do not appear in the formulation. Not only the maximum free-surface elevation amplitude but also the first order force was calculated. A general-purpose program for solving water wave problem by arbitrary number, size and various locations of cylinders was developed. The results were compared well with the approximate series solution of Linton and Evans and the plane wave BEM data by Perrey-Debain et al.

References

[1]   A.J. Burton and G.F. Miller, The application of integral equation methods to numerical solution of some exterior boundary value problems, *Proceedings of The Royal Society Series A*, Vol. 323, pp. 201-210, 1971.

[2]   H.A. Schenck, Improved integral formulation for acoustic radiation problem, *Journal of Acoustical Society of America*, Vol. 44, pp. 41-58, 1968.

[3]   J.T. Chen, K.H. Chen, I.L. Chen and L.W. Liu, A new concept of modal participation factor for numerical instability in the dual BEM for exterior acoustics, *Mechanics Research Communications*, Vol. 26(2), pp. 161-174, 2003.

[4]   A.F. Seybert and T.K. Rengarajan, The use of CHIEF to obtain unique solutions for acoustic radiation using boundary integral equations, *Journal of Acoustical Society of America*, Vol. 81, pp. 1299-1306, 1968.

[5]   T.W. Wu and A.F. Seybert, A weighted residual formulation for the CHIEF method in acoustics, *Journal of Acoustical Society of America*, Vol. 90(3), pp. 1608-1614, 1991.

[6]   L. Lee and T.W. Wu, An enhanced CHIEF method for steady-state elastodynamics, *Engineering Analysis with Boundary Elements*, Vol. 12, pp. 75-83, 1993.

[7]   S. Ohmatsu, A new simple method to eliminate the irregular frequencies in the theory of water wave radiation problems, Papers of Ship Research Institute 70 (1983).

[8]   I.L. Chen, Using the method of fundamental solutions in conjunction with the degenerate kernel in cylindrical acoustic problems, *Journal of Chinese Institute of Engineers*, Vol. 29(3), pp. 445-457, 2006.

[9]   E. Dokumaci and A.S. Sarigül, Analysis of the near field acoustic radiation characteristics of two radially vibrating spheres by the Helmholtz integral equation formulation and a critical study of the efficacy of the CHIEF over determination method in two-body problems, *Journal of Sound and Vibration*, Vol. 187(5), pp. 781-798, 1995.

[10] C.M. Linton and D.V. Evans, The interaction of waves with arrays of vertical circular cylinders, *Journal of Fluid Mechanics*, Vol. 215, pp. 549-569, 1990.

[11] M. Kitahara, *Boundary integral equation methods in eigenvalue problems of elastodynamics and thin plates*, Amsterdam: Elesvier, 1985.

[12] A.Z. Elsherbeni and M. Hamid, Scattering by parallel conducting circular cylinders, IEEE Trans. Antennas. Propag. 35 (1987) 355-358.

[13] M.J. Grote and C. Kirsch, Dirichlet to Neumann boundary conditions for multiple scattering problems, *Journal of Computational Physics*, Vol. 201, pp. 630-650, 2004.

[14] R. Kress, *Linear integral equations*, Berlin: Springer-Verlag, 1989.

[15] R. Kress, On the numerical solution of a hypersingular integral equation in scattering theory, *Journal of Computational and Applied Mathematics*, Vol. 61, pp. 345-360, 1995.

[16] E. Perrey-Debain, J. Trevelyan and P. Bettess, Plane wave interpolation in direct collocation boundary element method for radiation and wave scattering: numerical aspects and applications, *Journal of Sound and Vibration*, Vol.261, pp.839-858, 2003.

[17] L.C. Wrobel, T*he boundary element method Vol. 1, Applications in Thermo-Fluids and Acoustics*, New York: John Wiley, 2002.

[18] J.T. Chen, W.C. Shen and A.C. Wu, Null-field integral equations for stress field around circular holes under antiplane shear, *Engineering Analysis with Boundary Elements*, Vol. 30, pp. 205-217, 2006.